applied sciences

MDPI

Article

Study on Microwave Deicing of Carbon-Fiber-Modified Concrete under Multi-Factor Coupling Effect

He Huang [1], Jinyu Xu [1,2], Ao Yao [1,*], Wei Xia [1], Erlei Bai [1] and Yipeng Ning [1]

[1] School of Aeronautical Engineering, Air Force Engineering University, Xi'an 710038, China; huangheafeu@163.com (H.H.); xiaweiafeu@163.com (W.X.); xujinyuafeua@163.com (J.X.); baierleiafeu@163.com (E.B.); ningyipeng1998@163.com (Y.N.)

[2] College of Mechanics and Civil Architecture, Northwest Polytechnic University, Xi'an 710072, China

* Correspondence: yaoaokgd@163.com; Tel.: +86-155-9660-4972

Abstract: To explore the law of microwave deicing of carbon-fiber-modified concrete under the action of multiple factors and improve its application in pavement, in this study, we designed a test of the heat absorption and deicing effect of concrete under the action of multiple factors. We found that the law of heat absorption and deicing of CFRP is influenced by the coupling effect of fiber length and dosage, height (straight-line distance between the microwave receiving surface and bell component), initial temperature and ice cover. The temperature rises fastest when the fiber dosage is 0.2% and fiber length is 6 mm without ice. Further analysis of other factors shows that the deicing effect is optimal when the height is 40 mm, and the presence of ice on fiber-reinforced concrete weakens the microwave deicing efficiency, although the reduction is small. The test results of these two factors are in agreement with the simulation results and conform to expectations. The initial temperature has a considerable influence on the deicing efficiency. In practical applications, the deicing time should be adjusted according to the initial temperature in order to prevent the phenomenon of secondary icing when the heating time is too long. Based on heat generation and heat dissipation, the four stages of microwave deicing were analyzed, and the relationship with the temperature increase rate was deduced. It was proven that carbon fiber affected the deicing efficiency by changing the microwave absorption and reflection effect of concrete.

Keywords: carbon-fiber-modified concrete; microwave deicing; electromagnetic wave simulation calculation

Citation: Huang, H.; Xu, J.; Yao, A.; Xia, W.; Bai, E.; Ning, Y. Study on Microwave Deicing of Carbon-Fiber-Modified Concrete under Multi-Factor Coupling Effect. *Appl. Sci.* **2022**, *12*, 5551. https://doi.org/10.3390/app12115551

Academic Editor: Chao-Wei Tang

Received: 9 May 2022
Accepted: 26 May 2022
Published: 30 May 2022

1. Introduction

1.1. Research Background

To meet the increasing demand for transportation at high latitudes and high altitudes, an increasing number of airports are being built in areas with special climatic conditions, resulting in problems caused by snowfall and other factors [1,2]. Ice on airport runways has become a key consideration with regard to the safety and efficiency of aircraft taking off and landing in alpine regions [3].

Common deicing methods used to resolve surface ice and reduce the tire and road surface friction coefficient [4,5] include mechanical deicing and two kinds of chemical deicing methods. Mechanical deicing refers to the use of human labor or equipment to physically break ice, followed by removal and collection of the broken ice. Mechanical deicing is a mainstream method of ice removal and can quickly remove ice on road surfaces after icing with excellent results. However, it takes a long time to remove ice, resulting in high labor costs, and mechanical deicing can cause damage to road surfaces and reduce the flatness of the airport road surface [6,7]. Chemical deicing is a specialized method of deicing achieved by reducing the freezing point of water to prevent ice formation. However, most chemical deicing agents are salt ion compounds [8], and the corrosion effect of such

ions dissolved in water on concrete also affects the durability and service life of the runway surface layer.

Therefore, researchers have focused on improving the efficiency of active deicing and eliminating the impact on the concrete surface. The traditional heating method involves heat the ice layer and concrete surface layer at the same time [9,10], which is inefficient and requires a long heating time [11,12]. As the main heating method, microwave deicing can transfer most of the energy to the concrete [13]. The ice absorbs less energy to achieve a heating effect, which considerably improves the deicing efficiency.

Xu et al. [14–18] performed a systematic analysis of various factors in microwave deicing. In terms of height [14], it was found that an increase in microwave source height increased the absorption heat uniformity of carbon fiber concrete and reduced the heating rate. Graphite, iron black and other materials were added to concrete [15,16], which increased the deicing rate by 5.1 times and the dielectric constant by 3.5~4.7 times. In terms of mixed modified materials [17,18], graphite and iron black were mixed together, and the deicing efficiency was measured and compared. The deicing rate was the fastest when concrete was mixed with another substance, reaching 0.61 °C/s. Gao et al. [19–21] studied the microwave performance of steel-fiber-modified concrete and steel slag-waste-modified concrete mixed with asphalt; all their studies revealed that the addition of modified materials with good electrical conductivity considerably improved the deicing efficiency of concrete. Ding et al. [22,23] took microwave deicing sources as the main research object and studied the deicing heating efficiency of electromagnetic waves with different frequencies. Their study showed that when the microwave frequency was 2.45 ghz, the addition of a Fe-Al mixture with a mass ratio of 1% was optimal; when the microwave frequency was 5.8 ghz, the addition of iron-hydroxyl iron powder with a mass ratio of 5% was found to be optimal. Meng et al. [24] took carbon-fiber-modified concrete as a research object and analyzed its absorption performance. Their study showed that the longer the carbon fibers, the higher the heating efficiency and heating rate of concrete. Wang et al. [25,26] used the coarse aggregate in modified concrete as an entry point to change the original wave-absorbing properties of concrete and conducted a wave absorbance study on magnetite concrete, which showed that ice thickness had little influence on the deicing performance of different kinds of coarse aggregate concrete.

1.2. Research Significance

To date, few factors have been considered in the study of microwave deicing of concrete. There are many factors to be considered in the microwave deicing process. Variation of factors affects deicing efficiency, which has research value for the study of the microwave deicing effect of carbon fiber concrete under the combined effect of multiple factors.

We studied the law of deicing caused by the temperature rise of carbon-fiber-modified concrete absorbing electromagnetic waves. Carbon fiber modification on the surface of concrete in cold areas (airport applications) to improve deicing efficiency, as well as the geographical location of the airport, can, to a certain extent, resolve the issue of concrete surface ice for planes landing and taking off so as to ensure the normal operation of the airport and to solve the problem of insecurity caused by ice on airport road surfaces in high-altitude and high-latitude areas.

1.3. Research Program

In this study, carbon fiber concrete with different dosages (0, 0.1%, 0.3% and 0.6%) and lengths (3 mm and 6 mm) was prepared, and the height of a microwave transmitter was used to set the test control group (20 mm, 40 mm and 60 mm). Under the coupling of the two parameters of the ice layer on the surface of the concrete and the initial temperature, a multi-factor coupling test was carried out with carbon fiber, ice, microwave height factor and initial temperature as variables, and the overall temperature of the concrete surface was analyzed. COMSOL Multiphysics software was used to simulate and verify the accuracy and regularity of the experiments.

2. Materials and Methods

2.1. Raw Materials

The material used in this test is ordinary Portland cement (P·O) produced by Leish Brothers Company in Hangzhou, with a density of 3.0 g/cm^3, a fineness of 1.7 and specific surface area of 340 m^2/kg. The main chemical components of silica, calcium oxide and aluminum oxide accounted for 23.14%, 61.57% and 5.73%, respectively. Gravel from Yongshun Stone Processing Plant in Shijiazhuang city, Hebei Province, was selected as fine aggregate, with a fine aggregate density of 2.51 g/cm^3 and a bulk density of 1.48 g/cm^3. The coarse aggregate density was 2.75 g/cm^3, and bulk density was 1.68 g/cm^3, comprising a mixture of coarse aggregate medium gravel (20–40 mm), medium- gravel (10–20 mm) and small gravel (5–10 mm) in a ratio of 1:1:0.5. After full mixing, the mud content of the two aggregates was less than 0.4%. In this experiment, we used carbon fiber produced by Youlida Company, China. The diameter of the carbon fiber was 8 μm, with tensile strength of 3 GPa, carbon content of 95%, Young's modulus of 228 GPa and resistivity between 1.2 Ω·cm and 1.6 Ω·cm, as shown in Figure 1.

Figure 1. Basic morphology of carbon fiber after cutting.

In the pouring process, concrete was prepared with a self-made model of 500 × 500 × 10 mm, which was maintained by standard curing method.

To prepare concrete covered with ice, insert the upper part of the cured concrete specimen into the marked scale indicator ruler, place the central and edge portions of the concrete into the temperature sensor, and water the concrete in 3 batches. The watering depth of a single time is controlled from 30 mm to 40 mm. After watering, transfer the sample to cold storage (−10 ± 1 °C) for 4 h and repeat the above steps to achieve the desired ice thickness.

In Figure 2, part 1 and part 2 show temperature measuring devices for the central point position and the edge point position, respectively, and 4 identifies the ruler with marker scale.

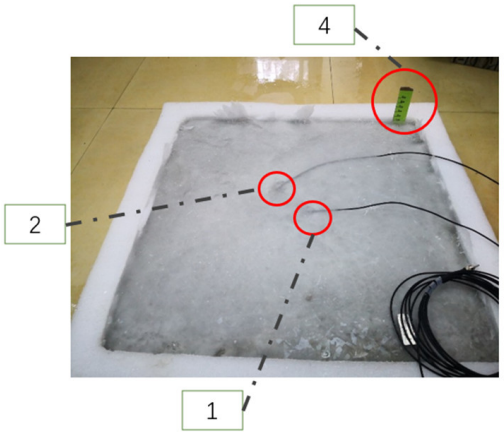

Figure 2. A concrete specimen covered with ice.

For the experiment, we used microwave instruments with an independent microwave launcher joint structure design. In Figure 3, part 5 shows the microwave source selection produced by the Samsung ESGN model, with a transmitter microwave frequency of 2.45 GHz, and 6 and 7 identify the microwave component microwave diffusion trumpet, respectively, which were the target for the uniform microwave irradiation test.

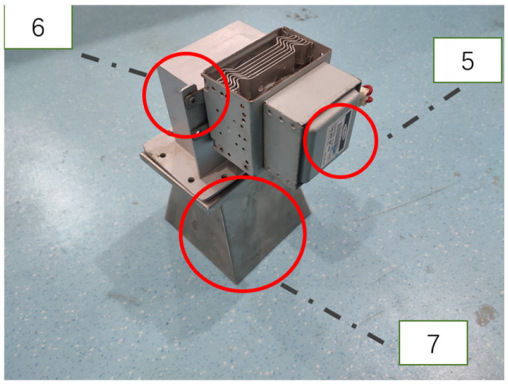

Figure 3. Microwave emission source unit.

2.2. Test Equipment and Method

As shown in the Figure 4, 1 is the temperature measurement instrument for the edge of the concrete, 2 is the temperature measurement instrument for the center of the concrete, 3 is the microwave generated when the microwave-transmitting device is in operation, and 4 is the ruler with marker scale.

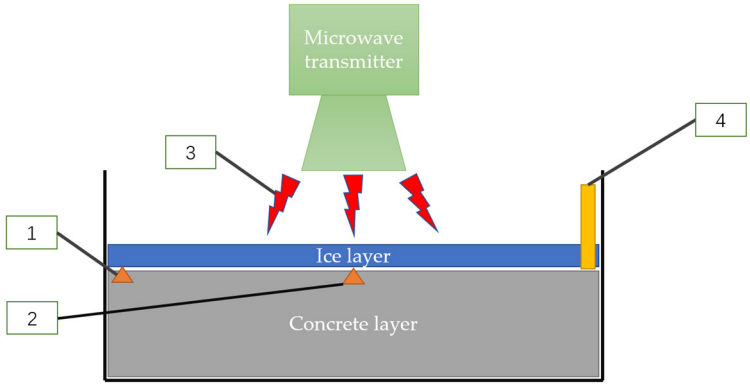

Figure 4. Schematic diagram of the basic test device.

The lower trumpet of the microwave emitter and the surface height of the specimen were set as 20 mm and 40 mm, respectively, and the length and dosage of carbon fiber were shown in Table 1.

Table 1. Microwave deicing test group.

Test Number	Fiber Length	Fiber Content
PC	0	0
0.1 CFC3	0.1 mm	0.3%
0.3 CFC3	0.3 mm	0.3%
0.6 CFC2	0.6 mm	0.2%
0.6 CFC3	0.6 mm	0.3%

The absorbance and heating efficiency of different carbon-fiber-modified concrete samples was tested. The concrete surface was not covered with ice in this test.

At the end of the first test, 0.6 CFC3 carbon-fiber-modified concrete was prepared, and a 10 cm ice layer was deposited on its top surface. A second test was carried out for deicing of the ice layer with heating at different heights.

On this basis, the third test was carried out on 0.6 CFC3 CFRP specimens at different initial temperatures of −10 °C, −6 °C and −2 °C with a 10 mm thick ice layer.

The temperature acquisition instrument used in the test was an optical fiber thermometer, and the temperature–time variation curves of the center point (T_0) and the edge point (T_1) on the surface of the concrete specimen were obtained.

3. Results

3.1. Effects of Carbon Fiber Content and Length on Heating Temperature

Five groups of ice-free concrete specimens (PC, 0.1 CFC3, 0.3 CFC3, 0.6 CFC2 and 0.6 CFC3) were subjected to a wave absorption heating test. The temperature–time curve and the temperature-change-rate–time curve of the five groups of specimens are shown in the Figures 5 and 6, from which the following conclusions can be drawn:

(1) In the same group of specimens, with increased height (straight-line distance between microwave receiving surface and bell-mouth component), the temperature rises gradually and then decreases. When the vertical height is 20 mm, the absorbing heat efficiency is the highest. The increase in temperature amplitude of the PC group was higher than 40 mm when the microwave source height was 60 mm, and that of 0.6 CFC2 was 20 mm when the microwave source height was 40 mm. This indicates that the optimal heating height of concrete varies depending on the length and content of carbon fibers used for modification, and there is no optimal height suitable for all concrete materials. At the same height, the temperature of the specimen increases in a process of dynamic stability; the optimal carbon fiber length and content of the modified concrete are not affected by heating height, but these parameters affect the heating efficiency.

(2) When the height was 20 mm, the rate of temperature increase of 0.6 CFC2 and 0.6 CFC3 varied considerably, and the temperature increase rates of the two test groups fluctuated to a certain extent. The other test groups, such as PC, 0.1 CFC3 and 0.3 CFC3, all reached a plateau, and the temperature rose steadily from 20 s to 40 s. Therefore, with increased height, the temperature increase rate of 0.6 CFC2 and 0.6 CFC3 specimens emerged as stable, showing that carbon fiber modification of concrete in the process of microwave heating increase the temperature rate fluctuation to stable value relative to carbon fiber content and fiber length. Regardless of the height, the shape of the temperature increase rate curve first increases rapidly and then tends toward a stable value.

(3) When the height is 20 mm, the temperature increase at the central point (T_0) of the PC specimen is 32.3 °C, that of the 0.6 CFC2 specimen is 61.4 °C, and the absorption and heating efficiency are increased by 1.90 times. When the height of the microwave source trumpet is 40 mm, the temperature increase of the PC specimen is 20.4 °C, and that of 0.6 CFC2 is 53.0 °C, representing an increase of about 2.60 times. This indicates that carbon fiber has a more obvious improvement effect on the ice-free wave absorption heat performance of concrete at a height of 40 mm for the 0.6 CFC2 specimen, which is the best performance in the test group.

(4) Overall, height has a considerable influence on the absorption and heating performance of CFRP. For the same specimen, the temperature increase at a height of 20 mm is about 1.5 to 2 times higher than that at a height of 60 mm. Our results are consistent with those reported in a study by Meng [24] on the wave-absorbing and heat-generating properties of concrete with different carbon fiber lengths, confirming that longer carbon fiber length results in improved wave-absorbing and heat-generating properties of modified concrete.

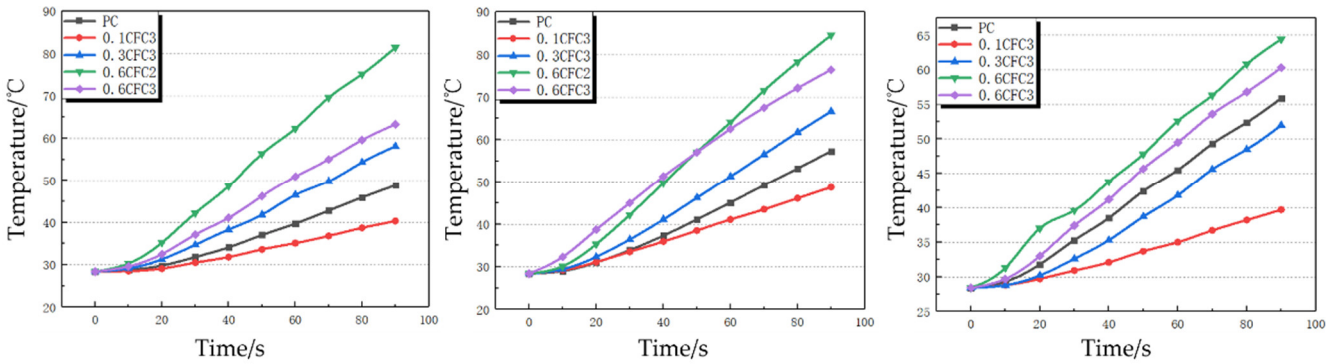

Figure 5. Temperature increase curve at the center point (T_0) of modified concrete samples with different carbon fiber contents and lengths.

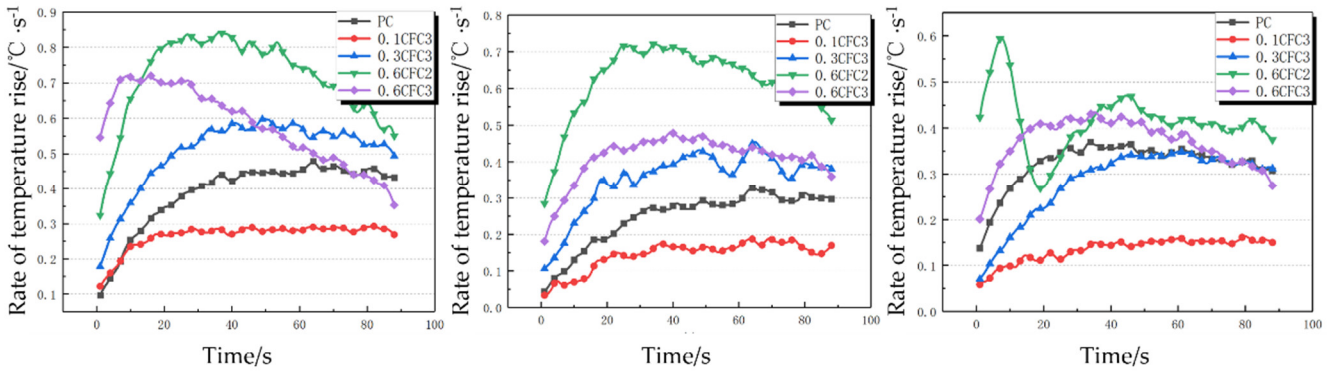

Figure 6. Temperature increase rate at the center point (T_0) of modified concrete with different carbon fiber contents and lengths.

3.2. *Effect of Microwave Irradiation Height on Deicing*

Based on the above ice-free test, 0.6 CFC3 specimens were selected for deicing tests under microwave irradiation at different heights (10 mm, 20 mm, 40 mm and 60 mm). The ice thickness on the upper surface of the specimens was maintained at 10 mm, and the temperature increase curves and deicing effects were obtained at four heights. The results are shown in the Figures 7–9. Regardless of the height, the inflection point of the temperature increase curve is about 50 s, i.e., the water layer is completely formed, indicating that the height does not affect the time to form a complete water layer on the concrete pavement. Because the time to form a water layer on concrete is considerably affected by the absorption and heat performance of water, the height has a considerable influence on the absorption and heat performance of carbon fiber concrete but has little influence on the absorption and heat performance of water. As the height increases, the temperature gradually increases, reaching its maximum value when the height is 40 mm. In the first half of the temperature increase curve, the temperature change rule under the height of 20 mm is similar to that under the height of 40 mm. However, after 85 s, the temperature at the center point (T_0) on the surface of the specimen with a height of 40 mm increases significantly, indicating that the deicing efficiency is better at a height of 40 mm. There was no obvious deicing effect on the highly irradiated specimen surface, especially with a microwave source height of 40 mm. When the temperature was increased to 34 °C, ice did not form, indicating a good deicing effect on the 0.6 CFC3 specimen and a more horizontal temperature transfer, as opposed to vertical heating of the ice. The temperature change results obtained in this experiment are similar to those reported by Xu et al. with respect to heating height in absorbance tests [14] for deicing of carbon fiber concrete on the basis of a microwave frequency of 2.45 GHz.

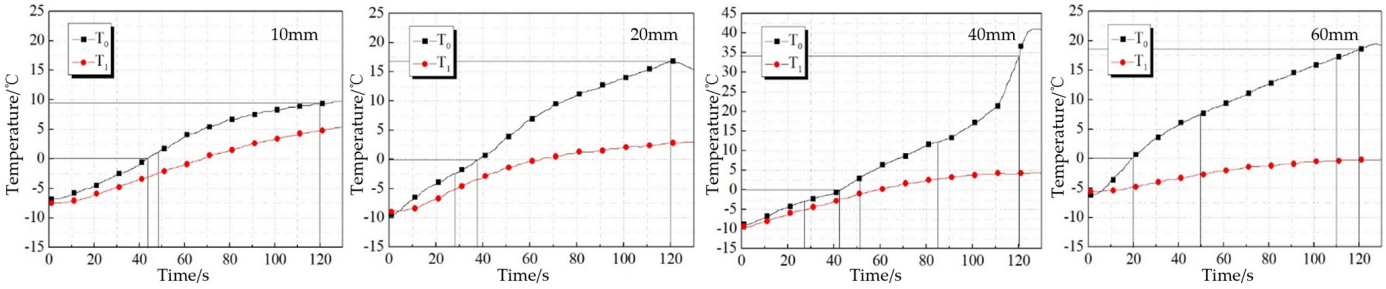

Figure 7. Temperature curves of specimens at different heating heights over time.

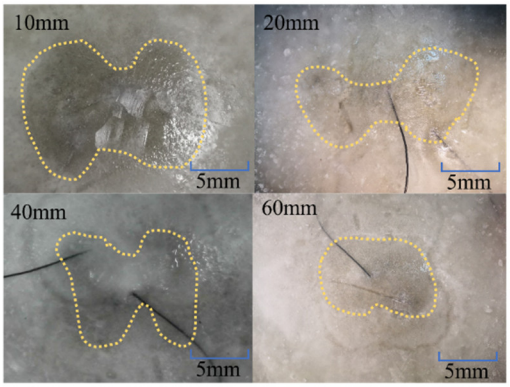

Figure 8. Deicing effect of specimens at different heights.

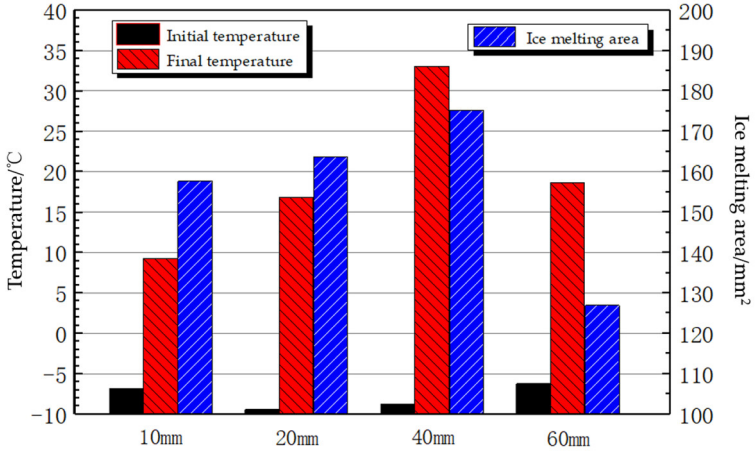

Figure 9. Temperature increase rate at the center point (T_0) of concrete specimens with different carbon fiber contents and lengths.

For further comparison, the deicing area was measured at different heights. With increased height, the shape of the deicing area gradually changed from a dumbbell shape to an oval shape; the width of the center line gradually increased; the width of the left and right semicircles gradually decreased; and the ratio of the width of the left and right semicircles to the width of the center line gradually decreased. When the height is 10 mm, the width of the middle line is 6.39 cm, the width of the left semicircle is 12.06 cm and the width ratio is 1.89. When the microwave source trumpet height is 20 mm, the ratio decreases to 1.51. When the height of microwave source trumpet is 40 mm, the ratio decreases to 1.08, and the width is almost the same. When the height is 60 mm, the width of the center line is larger than the length of the center line for the first time, and the absorbing heating surface is oval. Therefore, from the perspective of shape, at a microwave source trumpet height of 40 mm, the shape of the deicing area approximates a rectangle under the irradiation of multiple microwave emission sources, resulting in an improved arrangement of the deicing

position. With increased height, the deicing area first increases first and then decreases. When the height of the microwave source trumpet is 40 mm, the deicing area reaches a maximum of 175.24 cm^2, and when the height of the microwave source trumpet is 60 mm, the deicing area is 126.88 cm^2. At a height of 40 mm, the deicing area is 1.38 times that at a height of 60 mm. Therefore, from the point of view of deicing area, the deicing effect is improved when the height of the microwave source trumpet is 40 mm. When the height is 40 mm, the temperature increase curve rises sharply after the formation of a water layer because the deicing area is further expanded at this time, i.e., after the initial formation of a water layer, the absorbed heat is more transversely transmitted to separate the ice sheet from the channel surface rather than longitudinally transmitted to thin the ice sheet. This is consistent with the conclusion that the deicing area at a height of 40 mm is much larger than that at other heights. By observing the relative position of the temperature measuring point (T_1) and the deicing area of the edge point in the deicing area diagram, it can be seen that the edge line of the deicing area is the isotherm of the temperature at 0 °C on the surface of the specimen. When the microwave source height is 20 mm, T_1 is located inside the deicing area, which corresponds to a final temperature of 5 °C at T_1, which is higher than 0 °C. When the microwave source height is 60 mm, T_1 is located at the edge of the deicing area, which corresponds to a final temperature of exactly 0 °C. Therefore, the edge line of the deicing area is the isotherm of 0 °C, which also indicates that the deicing operation can start when the specimen surface reaches 0 °C.

3.3. Effect of Initial Temperature on Deicing

With a height of 20 mm and after continuous irradiation for 120 s, 0.6 CFC3 carbon fiber concrete specimens were tested at −10 °C, −6 °C and −2 °C; the temperature changes of each specimen are shown in Figure 10.

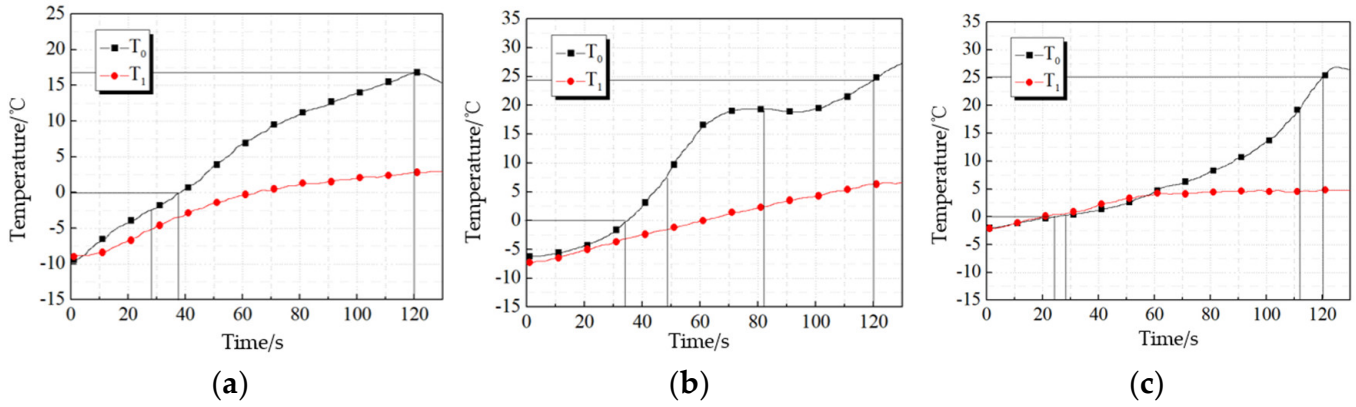

Figure 10. Temperature changes of each specimen at different initial temperatures. (**a**) −10 °C; (**b**) −6 °C; (**c**) −2 °C.

It can be seen from the Figures 10 and 11 that (1) when the initial temperature was −10 °C, −6 °C and −2 °C, the final temperature of the central point (T_0) after microwave heating for 120 s was 17.2 °C, 24.9 °C and 26.3 °C, respectively. The time for the temperature of the central point (T_0) on the surface of the specimen to reach 0 °C was 40 s, 33 s and 24 s, respectively. This indicates that the higher the initial temperature, the shorter the time for the specimen to reach 0 °C, the shorter the deicing time and the faster the deicing speed. The deicing speed of the specimen at −2 °C was about 1.7 times of that at −10 °C. (2) When the initial temperature was −10 °C, −6 °C and −2 °C, the deicing areas were 163.73 cm^2, 181.45 cm^2 and 232.93 cm^2, respectively. With a higher initial temperature, the deicing area was larger with the same deicing time. When the initial temperature was 2 °C, the deicing area was significantly larger than with an initial temperature of −10 °C of 6 °C; this is because the initial temperature not only improves the center of the specimen surface (T_0) but also the initial temperature of the ice. Therefore, a higher initial temperature can

significantly increase the efficiency of deicing. (3) When the initial temperature was −10 °C, the temperature at the center point (T_0) on the surface of the specimen reached 0 °C after heating for 40 s, with no plateau near 0 °C on the temperature increase curve, and the last ice sheet did not break, indicating that the temperature increase rate in the central region was fast, and the initial melting area was small. Once the temperature reached 0 °C, a water layer formed quickly and melted the ice sheet, acting as a heat source. However, because the heat is spread more sideways than upward, the ice did not break, and there was no fluctuation in the rate of temperature increase. (4) When the initial temperature was −6 °C, the temperature increase curve of the central point (T_0) reached 0 °C after 33 s of heating, and there was no plateau at 0 °C, indicating that a water layer formed quickly. With a higher initial temperature, the ice is easier to melt, and it takes less time to reach 0 °C, so the temperature of the central point (T_0) remains near 20 °C for a long time after 60 s of heating. A plateau appeared in the temperature increase curve, and the temperature increase rate reached its lowest value, indicating that the ice broke at this time and that the temperature increase rate sharply decreased before ice breaking, which is consistent with the previous theoretical derivation.

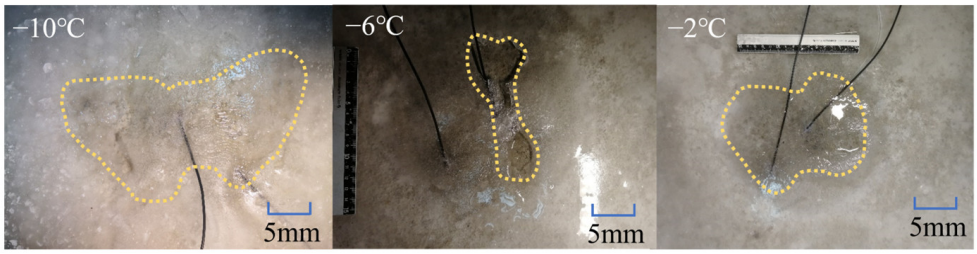

Figure 11. The actual deicing effect of each specimen at different initial temperatures.

In conclusion, varying initial temperatures have a similar effect as different starting points of the same heating process. Because the initial temperature affects the temperature of the ice, the higher the initial temperature, the smaller the temperature difference between the ice, water layer and concrete and the shorter the deicing time. The deicing time of a specimen at an initial temperature of −2 °C is only 60% of that of a specimen with an initial temperature of −10 °C. Therefore, in deicing operation on airport runways, it is necessary to control the deicing time according to the actual temperature of the ice. Improper control of deicing time may lead to wasted energy and even cause a large amount of melting, as well as an ice breaking phenomenon, resulting in secondary icing.

4. Simulation Experiment

In order to facilitate the computer simulation calculation, some unnecessary factors are simplified and assumed in the simulation process. The specific simplified conditions and assumed conditions are as follows:

(1) Thermal convection between ice and air is not considered. According to the theoretical analysis, the thermal convection between the ice layer and air is very limited, so it can be ignored. However, a boundary condition needs to be set for the thermal convection between the water layer and air after ice breaking. That is, after the ice is broken, the air is a poor conductor to the water layer.

(2) The whole simulation is set in a finite space, and the boundary of the space is set as a perfect matching layer; that is, it is assumed that there is no energy exchange between the space and the outside world, and microwave irradiation takes place in a completely adiabatic environment.

(3) The mixture of ice and water is taken as a whole, the combination values of the thermodynamic parameters of ice and water are considered and the change in the ratio of water and ice theta is realized to change the mixture parameters of the ice–water phase transition by temperature and other variables.

Based on the above three constraints, the constructed model can simulate the wave-absorbing heating process of different materials by changing the electromagnetic parameters of channel materials, simulate the ice thickness in a real environment by changing the ice thickness and can be used to simulate the microwave heating process without ice when the ice thickness is 0. The actual conditions of different microwave sources and the external environment are simulated by adjusting the height and initial temperature.

Open space can be used for simulation of an absorbance model with different materials, different heights, different thicknesses of the ice and different initial microwave temperatures. The simulation adopts a perfectly matched layer boundary and can therefore basically describe open space under the ice without a change in ice thickness and with a single microwave source.

The parameters of the model are shown in Figure 12: the size of the waveguide is 5.46 × 10.92 × 15 cm. The dimension parameters of the bell mouth are as follows: vertical wall height, oblique wall height, bottom opening width. The ice layer is 50 × 50 × 5 cm, and the concrete specimen is 50 × 50 × 5 cm. The height of the bell mouth from the concrete surface is measured in 15 cm. The size of the air environment is 100 × 100 × 100 cm, and an impedance matching layer is added to the outer edge of the air.

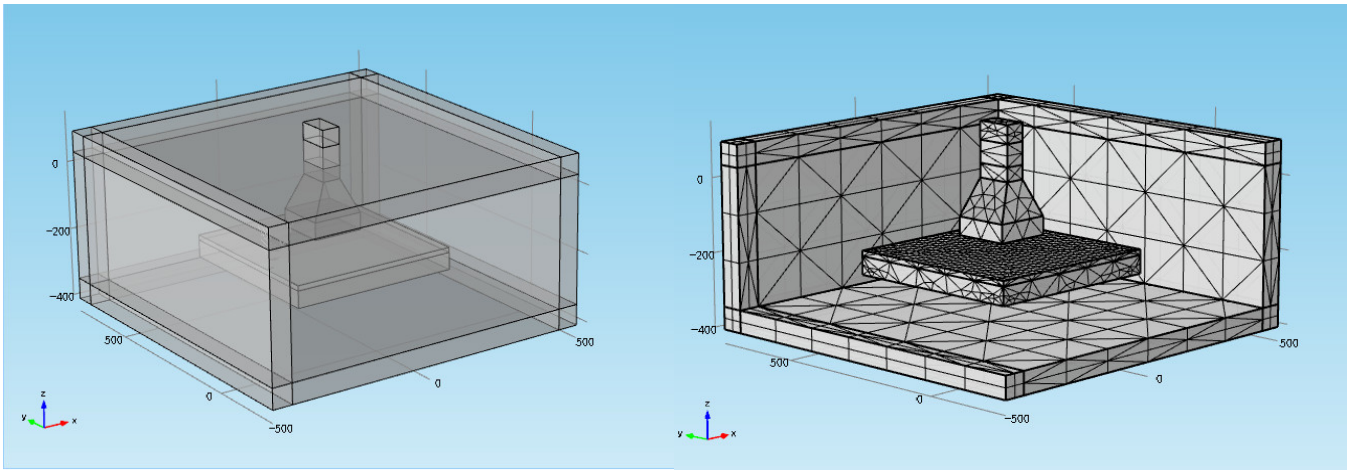

Figure 12. Schematic diagram of simulation grid construction.

Under the condition of no ice layer, the heat absorption efficiency of a concrete specimen with a height of 20 mm, 40 mm and 60 mm is simulated. The simulation results are as follows.

Under the condition of no ice layer, the heat absorption efficiency of a concrete specimen with a height of 20 mm, 40 mm and 60 mm is simulated. Figure 13 shows a geometric model diagram of different trumpet heights and a temperature distribution diagram of the concrete specimen surface after 90 s heating. According to Figure 13: (1) There is an obvious heating area on the concrete surface with a roughly oval shape, and the size of the heating area is similar to that of the trumpet. This shows that microwave can heat concrete and generate heat and that there is a clear area of heat generation. (2) The temperature increase at the central point (T_0) in the heating region is the highest, and the farther away from the central point (T_0), the lower the temperature increase. This shows that microwave heating is radiative, so multiple microwave sources can be used for channel heating to achieve multi-wave source coupling heat generation. (3) When the height is 20 mm, the area of the concrete surface temperature increase reaches 317.2 cm^2. Compared with a concrete surface area of 103.9 cm^2 in the test group with a height of 60 mm, the overall temperature increase area of the concrete surface decreases by 67.24% when the height is increased by 40 mm.

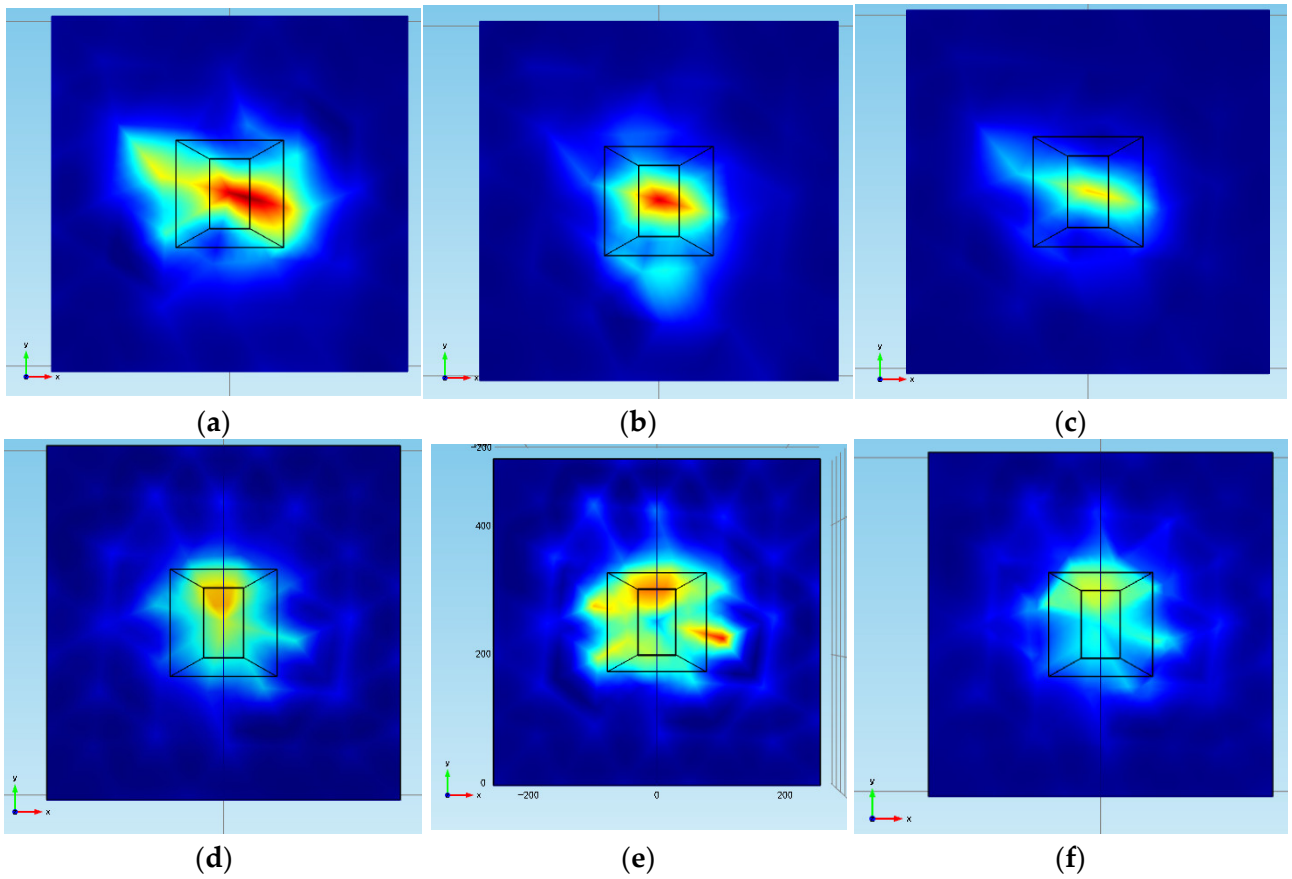

Figure 13. Simulation results of different ice layers and heights. (**a**) 20 mm, no ice; (**b**) 40 mm, no ice; (**c**) 60 mm, no ice; (**d**) 20 mm, no ice; (**e**) 40 mm, no ice; (**f**) 60 mm, no ice.

Ice–water phase change material is installed on the surface of the concrete, and the wave-absorbing and deicing performance of concrete specimens at heights of 20 mm, 40 mm and 60 mm is studied. The corresponding surface temperature distribution diagram of concrete is obtained (as show in Figure 13). It can be seen from the figure that: (1) There is an obvious elliptical heating area on the surface of the concrete, and the size of the heating area is similar to that of the bell mouth. This is similar to the result without ice, indicating that microwaves can penetrate ice and heat concrete and that the heating mechanism is similar to that without ice. (2) With the increase in microwave source trumpet height, the temperature increase range of T_0 at the center of the concrete surface first increases and then decreases. When the heating height is 40 mm, the temperature increase range is the largest, and the heating area reaches 253.7 cm^2. When the ice layer is 10 mm thick, the optimal heating height for deicing is 40 mm. (3) With the same heating height, compared with the ice and ice-free temperature ranges, the concrete surface temperature is not affected because the ice absorbs a lot of heat, reducing the temperature increase of the concrete surface.

5. Discussion

The reflection and absorption of microwave are selective. When encountering metal objects, a large number of reflections are generated, whereas when encountering insulating objects, most reflections are transmitted and continue to spread in the insulating body, resulting in loss of heat [15]. Therefore, when the microwave irradiates on concrete pavement with accumulated ice, it can directly irradiate the concrete through the ice, causing the concrete to heat up and melt the ice, weakening the binding force between the ice and concrete and achieving the effect of deicing. After microwave irradiation on the surface of the concrete specimen, the free electrons in the conductor inside the concrete move, and a charge appears on the surface of the conductor, resulting in an electric field equal

to and opposite to the applied electric field, which is called electrostatic balance. When the microwave acts on the surface of the conductor, due to the high frequency conversion of the applied electric field, the surface of the conductor forms an oscillating current and continues to radiate outwardly. The macroscopic manifestation is reflected microwaves. An ideal conductor can reflect all the microwaves without transmitting wave insides [27].

When the applied electric field acts on the dielectric field, because the electrons are in a bound state, there are almost no free electrons, and only microscopic relative displacement can occur, resulting in a dipole field. The directional arrangement of the dipole produces an electric field inside the dielectric field in the opposite direction to the applied electric field, and the electric field is smaller than the external electric field, which is called dielectric polarization. Under the action of an external electric field, a dipole field is generated by relative displacement of positive and negative charge centers, which is also called displacement polarization (as show in Figure 14). Because positive and negative charge centers do not overlap, the polar molecule itself is a dipole. Under the action of an electric field, not only is the dipole vector further shifted and polarized, but the thermal motion state of the molecule is also aligned with the chaos from the opposite direction, which is called turning-direction polarization, also known as orientation polarization. When the frequency the microwave changes to 2.45 GHz, a dipole polarization lag occurs with a high-frequency electromagnetic field. This process requires a thermal motion and interactions between molecules, producing a large amount of friction, which causes the external electromagnetic field energy to oscillate. The energy is converted into internal energy, and the macroscopic properties of microwave energy can be converted into thermal energy, called polarization loss, which is the main microscopic factor of microwave heating [28].

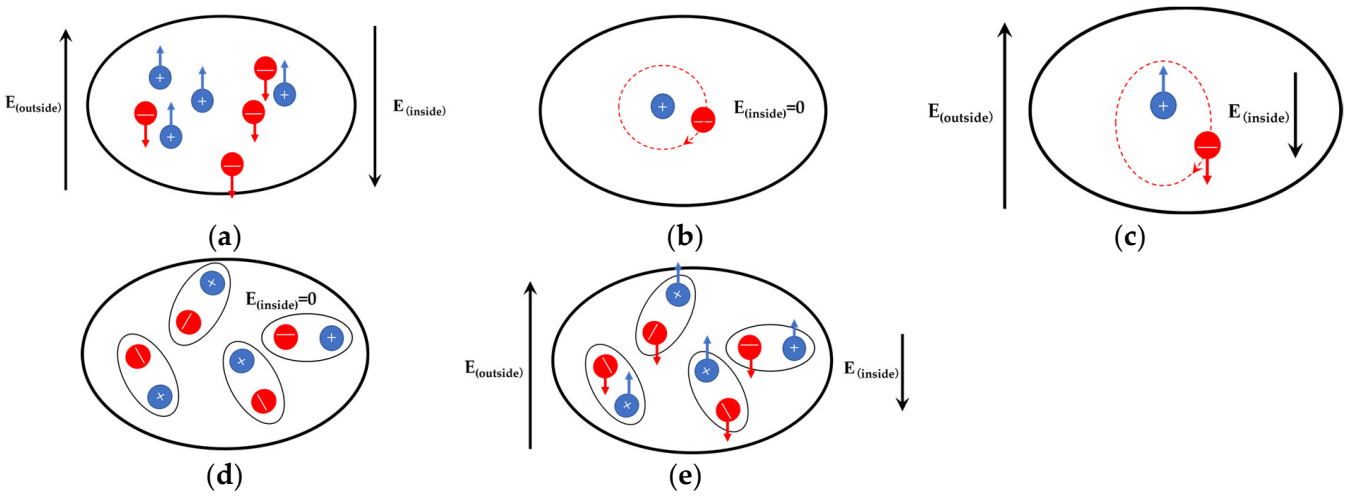

Figure 14. Simulation diagram of charge change in the conductor. (**a**) An external electric field acts on a conductor; (**b**) conductor internal displacement before polarization; (**c**) after internal displacement polarization of the conductor; (**d**) the conductor is oriented before polarization; (**e**) after the conductor is oriented and polarized.

After the polarization of the medium, polarization loss occurs, so that the power of the electromagnetic field gradually attenuates, and the electric field gradually decreases along the depth of the medium, converting microwave energy into heat energy. The electric field calculation Formula (1) is as follows:

$$E(x) = E_{\max} e^{j\omega t - \gamma x} \quad (1)$$

where $E_{\max}$ is the maximum electric field intensity of microwave refraction into concrete, which depends on the incident electric field intensity and reflectivity; and γ is the propagation coefficient, which depends on the complex permittivity and complex permeability.

The intensity of the electric field decays exponentially with depth in the medium. The decay rate depends on the complex dielectric constant and complex permeability of the dielectric material. The dissipated power of microwave absorption by a medium in a given space is related to the distribution of the electric field and the magnetic field in the space. The average dissipated power is usually calculated by the effective values of the electrical field and magnetic field, as shown in Formulas (2) and (3):

$$P_{av} = \omega\varepsilon_0\varepsilon''_{eff}E^2_{rms}V + \omega\mu_0\varepsilon''_{eff}H^2_{rms}V \tag{2}$$

$$\varepsilon''_{eff} = \varepsilon'' + \frac{\sigma}{\omega\varepsilon_0} \tag{3}$$

where ε'' is the imaginary part of the complex dielectric constant, representing the loss term in the polarization of the medium, reflecting the loss capacity of the medium, also known as the loss factor; σ is the conductivity of the medium; and ω is the circular frequency of the electromagnetic wave.

Therefore, a micro-element on the concrete surface is taken as the research object, and the heat generation rate of microwave absorption inside the micro-element is:

$$P_{av} = \frac{\mathrm{d}Q}{\mathrm{d}\tau} = cm\frac{\mathrm{d}T}{\mathrm{d}\tau} = c\rho V\frac{\mathrm{d}T}{\mathrm{d}\tau} \tag{4}$$

By substituting Formula (4) into Formula (2), Formula (5) is obtained as follows:

$$\frac{\mathrm{d}T_c}{\mathrm{d}\tau} = \frac{0.566\times10^{-10}}{c\rho}f\varepsilon''_{eff}E^2_{rms} \tag{5}$$

The temperature increase rate of a concrete surface under microwave irradiation is proportional to that of the concrete. Under the same conditions, a material with higher conductivity and lower reflectivity has a more significant wave-absorbing heating effect.

6. Conclusions

In this paper, a comprehensive study was conducted on the law of concrete wave absorption heat generation and deicing under the coupling effect of multiple factors, including carbon fiber dosage and length, microwave height, ice cover and initial temperature. The conclusions are as follows:

1. The incorporation of carbon fiber significantly improves the absorption and heating efficiency of concrete. After microwave irradiation, the overall heating area increases, and the temperature increase rate and range increase. The optimal fiber length is 0.6 cm, with 0.2% heating efficiency.
2. When the height of the microwave source trumpet is 40 mm, the deicing area and the temperature after deicing reach their maximum values, corresponding with the optimal height. The initial temperature and ice layer only affect the actual deicing effect but have little influence on absorption heating.
3. The simulation calculation results match the test results to a high degree, and the formation of the absorbing heating area is consistent with the actual heating area. The main factors affecting the absorption heating performance of carbon fiber concrete are the overall conductivity and microwave reflectance of the concrete. In this experimental study, we only considered a case of with single microwave source; for cases with multiple wave sources, further research is needed to establish a more widely applicable temperature increase analysis formula.

Author Contributions: Conceptualization, A.Y., W.X. and H.H.; methodology, A.Y., W.X. and H.H.; software, A.Y., W.X. and H.H.; validation, A.Y., W.X. and H.H.; formal analysis, A.Y., W.X. and H.H.; investigation, A.Y., W.X. and H.H.; resources, A.Y., W.X. and H.H; data curation, A.Y., W.X. and H.H.; writing—original draft preparation, A.Y., W.X. and H.H.; writing—review and editing, A.Y., W.X. and H.H.; visualization, A.Y., W.X. and H.H.; project administration, J.X., E.B. and Y.N. All authors have read and agreed to the published version of the manuscript.

Funding: This research was financially supported by the Natural Science Foundation of China (51908548) and the Youth Talent Promotion Program of Shaanxi University Association for Science and Technology (20200415).

Institutional Review Board Statement: The study did not involve humans or animals.

Informed Consent Statement: Informed consent was obtained from all subjects involved in the study. Written informed consent has been obtained from the patient(s) to publish this paper.

Data Availability Statement: The data used to support the findings of this study are available from the corresponding author upon reasonable request.

Acknowledgments: The authors express their thanks to all members of the laboratory team for their technical support.

Conflicts of Interest: The authors declare no conflict of interest.

References

1. Wesołowski, M.; Iwanowski, P. Apci evaluation method for cement concrete airport pavements in the scope of air operation safety and air transport participants life. *Int. J. Environ. Res. Public Health* **2020**, *17*, 1663. [CrossRef] [PubMed]
2. Koščák, P.; Berežný, Š.; Vajdová, I.; Koblen, I.; Ojciec, M.; Matisková, D.; Puškáš, T. Reducing the negative environmental impact of winter airport maintenance through its model design and simulation. *Int. J. Environ. Res. Public Health* **2020**, *17*, 1296. [CrossRef] [PubMed]
3. Smith, J.R. *Aircraft Performance Explanation and Concerns for Takeoff from a High Altitude Airport*; Central Missouri State University: Warrensburg, MO, USA, 2006.
4. Yager, T.J.; Phillips, W.P.; Horne, W.B.; Sparks, H.C. *A Comparison of Aircraft and Ground Vehicle Stopping Performance on Dry, Wet, Flooded, Slush-, Snow-, and Ice-Covered Runways*; National aeronautics and Space Administration Hampton va Langley Research Center: Washington, DC, USA, 1970.
5. Wang, L.W.; Yu, Z.J.; Zhang, L.; Gao, J.; Song, J.I. Study on the key technology of airport runway frictional coefficient measurement. In *Key Engineering Materials*; Trans Tech Publications Ltd: Bach, Switzerland, 2008; pp. 229–232.
6. Lichliter, A.; Faghri, A.; Li, M. Assessing airport snow and ice removal and its economic implications for sustainable airport management. *J. Airpt. Manag.* **2014**, *8*, 174–188.
7. Liu, F.; Meng, L.-y.; Ning, G.-F.; Li, L.-J. Fatigue performance of rubber-modified recycled aggregate concrete (rrac) for pavement. *Constr. Build. Mater.* **2015**, *95*, 207–217. [CrossRef]
8. Hassan, Y.; Abd El Halim, A.; Razaqpur, A.; Bekheet, W.; Farha, M. Effects of runway deicers on pavement materials and mixes: Comparison with road salt. *J. Transp. Eng.* **2002**, *128*, 385–391. [CrossRef]
9. Lai, Y.; Liu, Y.; Ma, D. Automatically melting snow on airport cement concrete pavement with carbon fiber grille. *Cold Reg. Sci. Technol.* **2014**, *103*, 57–62. [CrossRef]
10. Abdualla, H.; Ceylan, H.; Kim, S.; Mina, M.; Cetin, K.S.; Taylor, P.C.; Gopalakrishnan, K.; Cetin, B.; Yang, S.; Vidyadharan, A. Design and construction of the world's first full-scale electrically conductive concrete heated airport pavement system at a us airport. *Transp. Res. Rec.* **2018**, *2672*, 82–94. [CrossRef]
11. Abdualla, H.; Ceylan, H.; Kim, S.; Gopalakrishnan, K.; Taylor, P.C.; Turkan, Y. System requirements for electrically conductive concrete heated pavements. *Transp. Res. Rec.* **2016**, *2569*, 70–79. [CrossRef]
12. Pravda, M.; Trimmer, D.; Wolf, D. *Heating Systems for Airport Pavement Snow, Slush, and Ice Control*; National Technical Information Service: Springfield, VA, USA, 1975.
13. Gu, G.; Chen, F.; Ma, T.; Xu, F.; Yang, D. Electromagnetic and mechanical properties of soft magnetic cement composite for airport runway induction heating: Experimental and simulation analyses. *J. Clean. Prod.* **2022**, *332*, 130141. [CrossRef]
14. Chen, H.; Xu, J.; Wu, Y.; Liu, J.; Huang, H. Study on the thermodynamic properties of concrete surface during microwave deicing of airport pavement. *Materials* **2020**, *13*, 3557. [CrossRef]
15. Liu, J.-l.; Xu, J.-y.; Huang, H.; Chen, H. Microwave deicing efficiency and dielectric property of road concrete modified using different wave absorbing material. *Cold Reg. Sci. Technol.* **2020**, *174*, 103064. [CrossRef]
16. Liu, J.-l.; Xu, J.-y.; Lu, S.; Chen, H. Investigation on dielectric properties and microwave heating efficiencies of various concrete pavements during microwave deicing. *Constr. Build. Mater.* **2019**, *225*, 55–66. [CrossRef]
17. Lu, S.; Bai, E.; Xu, J.; Chen, J. Research on electromagnetic properties and microwave deicing performance of carbon fiber modified concrete. *Constr. Build. Mater.* **2021**, *286*, 122868. [CrossRef]

18. Lu, S.; Kong, L.; Du, J. Influence of microwave absorbing agents on microwave deicing of concrete road. *Int. J. Pavement Res. Technol.* **2022**. [CrossRef]
19. Gao, J.; Guo, H.; Wang, X.; Wang, P.; Wei, Y.; Wang, Z.; Huang, Y.; Yang, B. Microwave deicing for asphalt mixture containing steel wool fibers. *J. Clean. Prod.* **2019**, *206*, 1110–1122. [CrossRef]
20. Gao, J.; Sha, A.; Wang, Z.; Tong, Z.; Liu, Z. Utilization of steel slag as aggregate in asphalt mixtures for microwave deicing. *J. Clean. Prod.* **2017**, *152*, 429–442. [CrossRef]
21. Wang, H.; Zhang, Y.; Zhang, Y.; Feng, S.; Lu, G.; Cao, L. Laboratory and numerical investigation of microwave heating properties of asphalt mixture. *Materials* **2019**, *12*, 146. [CrossRef]
22. Ding, L.; Wang, X.; Cui, X.; Zhang, M.; Chen, B. Development and performance research of new sensitive materials for microwave deicing pavement at different frequencies. *Cold Reg. Sci. Technol.* **2021**, *181*, 103176. [CrossRef]
23. Ding, L.; Wang, X.; Zhang, W.; Wang, S.; Zhao, J.; Li, Y. Microwave deicing efficiency: Study on the difference between microwave frequencies and road structure materials. *Appl. Sci.* **2018**, *8*, 2360. [CrossRef]
24. Meng, X.; Bai, E.; Xia, W.; Huang, Z.; Wang, Z. Effect of Carbon Fiber on Microwave Deicing Efficiency of Pavement Concrete. In *IOP Conference Series: Earth and Environmental Science*; IOP Publishing: Bristol, UK, 2021; p. 032086.
25. Wang, Z.; He, Z.; Wang, Z.; Ning, M. Utilization of magnetite as microwave absorber to prepare microwave-heatable aggregate for deicing in cementitious composite. *Constr. Build. Mater.* **2019**, *227*, 116664. [CrossRef]
26. Wang, Z.; Wang, H.; An, D.; Ai, T.; Zhao, P. Laboratory investigation on deicing characteristics of asphalt mixtures using magnetite aggregate as microwave-absorbing materials. *Constr. Build. Mater.* **2016**, *124*, 589–597. [CrossRef]
27. Wang, Z.; Zhao, P.; Ai, T.; Yang, G.; Wang, Q. Microwave absorbing characteristics of asphalt mixes with carbonyl iron powder. *Prog. Electromagn. Res. M* **2011**, *19*, 197–208. [CrossRef]
28. Jie, G.; Zhengwei, Z.; Zhenqiang, H. Research progress of electromagnetic wave absorbing materials for microwave melting ice and snow pavement. *Mater. Rev.* **2016**, *30*, 87–95.